

# The Axis-Ratio Distribution of Galaxy Clusters in the SDSS-C4 Catalog as a New Cosmological Probe

JOUNGHUN LEE

*Astronomy Program, School of Earth and Environmental Sciences, Seoul National University, Seoul 151-742, Korea*

jounghun@astro.snu.ac.kr

## ABSTRACT

We analyze the C4 catalog of 748 galaxy clusters from the Sloan Digital Sky Survey (SDSS) to determine the axis-ratio distribution of their projected two dimensional profiles. It is found that the mean axis-ratio increases with cluster mass and luminosity, which is inconsistent with the result from N-body simulations where the cluster mean-axis-ratio decreases with mass. We also derive a theoretical axis-ratio distribution by incorporating the effect of projection onto the sky into the analytic formalism proposed recently by Lee, Jing, & Suto, and investigate how the theoretical distribution depends on the density parameter ( $\Omega_m$ ) and the amplitude of the linear power spectrum ( $\sigma_8$ ). Tested against the observational data from the SDSS-C4 catalog, the theoretical prediction is found to work quite well if the background cosmology is described by the concordance model. Finally, fitting the observational data to the analytic distribution with  $\Omega_m$  and  $\sigma_8$  as two adjustable free parameters, we find the best-fitting value of  $\sigma_8 = (0.99 \pm 0.07)\Omega_m^{(0.07 \pm 0.02) + 0.1\Omega_m}$ . It is a new  $\sigma_8$ - $\Omega_m$  relation, different from the previous one obtained with the local abundance of X-ray clusters. We expect that the axis-ratio distribution of galaxy clusters, if combined with the local abundance of clusters, may put simultaneous constraints on  $\sigma_8$  and  $\Omega_m$ .

*Subject headings:* cosmology:theory — large-scale structure of universe

## 1. INTRODUCTION

The standard theory of structure formation based on the cold dark matter (CDM) paradigm explains that the large scale structures of the universe like galaxies, groups and clusters of galaxies are originated from the primordial fluctuations of the matter density field

through gravitational instability. In this scenario, the observed properties of the large scale structures can be used to extract crucial informations on the initial condition of the early universe.

Among the various properties of the large scale structures, it is the abundance of galaxy clusters that has attracted most cosmological attentions so far. Since the clusters are relatively young still in the quasi-linear regime, their abundance can be inferred from the linear theory (e.g., Press & Schechter 1974). Furthermore, being rare, the evolution of galaxy clusters depends sensitively on the background cosmology, especially on the amplitude of the matter power spectrum on scale of  $8h^{-1}$  Mpc ( $\sigma_8$ ) and the density parameter ( $\Omega_m$ ). It has been shown that by comparing the linear theory prediction with the cluster abundance from X-ray or Sunyaev-Zel'dovich (SZ) effect observations one can constrain  $\sigma_8$  and  $\Omega_m$  (White, Efstathiou, & Frenk 1993; Bond & Myers 1996; Eke, Cole, & Frenk 1996; Pen 1998; Henry 2000; Fan & Chiueh 2001; Pierpaoli, Scott, & White 2001; Seljak 2002). For instance, Eke, Cole, & Frenk (1996) found a relation of  $\sigma_8 = (0.52 \pm 0.04)\Omega_m^{-0.52+0.13\Omega_m}$  (for a flat universe with non-zero cosmological constant,  $\Lambda$ ) by comparing the Press-Schechter prediction with the local abundance of the X-ray clusters compiled by Henry & Arnaud (1991).

To break the degeneracy between  $\sigma_8$  and  $\Omega_m$ , however, it will be necessary to find another relation obtained from another observable property of galaxy clusters. One candidate is the shapes of galaxy clusters.

The cluster shape was conventionally assumed to be spherical. But, recent numerical simulations (Jing & Suto 2000; Hopkins, Bahcall & Bode 2005) as well as observations demonstrated clearly that the galaxy clusters in fact have elliptical shapes. Furthermore, it was also shown by numerical simulations that the ellipticity distribution of galaxy clusters depend strongly on the background cosmology. This numerical finding implies that it may be possible to find a new independent relation between  $\Omega_m$  and  $\sigma_8$  with the ellipticity distribution of galaxy clusters.

Most of the previous approaches to the cluster ellipticity distribution were numerical. In order to use the cluster ellipticity distribution as a cosmological probe, however, it is highly desirable to have an analytic model for it derived from physical principles. Although Bardeen et al. (1986) made a first analytic attempt in the frame of the density peak formalism, their model was applicable only in the asymptotic limit of low ellipticity.

Very recently, Lee, Jing, & Suto (2005, hereafter, LJS05) derived a new analytic expression for the halo axis-ratio distribution by combining the density peak formalism and the Zel'dovich approximation. They demonstrated that the analytic model produced the characteristic behaviors of the halo axis-ratio distribution found in simulations, which gives a hope

that it may provide a theoretical footing for the use of the cluster ellipticity distribution as a cosmological probe, although it has yet to pass N-body tests on galaxy cluster scale (see §5).

Our goal here is to find a new functional form of the  $\sigma_8$ – $\Omega_m$  relation, independent of the one obtained previously from the cluster abundance, by comparing the LJS05 analytic prediction with the axis-ratio distribution of galaxy clusters determined from the recent observational catalog. The plan of this paper is as follows: In §2, we provide a brief description of the observational data. In §3, we explain how to derive an analytic axis-ratio distribution of two dimensional projected profiles of galaxy clusters from the LJS05 formalism. In §4, we find a new functional form of relation  $\sigma_8$ – $\Omega_m$  relation through application of theory to observation. §5, we discuss the caveat of our results, and draw a final conclusion.

## 2. DATA FROM SDSS-C4 CATALOG

We use the C4 catalog of 748 galaxy clusters (Miller et al. 2005) identified in the Second Data Release (DR2) of the Sloan Digital Sky Survey (SDSS, Strauss et al. 2002). The sky coverage and the redshift range of the catalog are  $\sim 2600 \text{ deg}^2$  and  $0.02 \leq z \leq 0.17$ , respectively. The majority of the objects in this catalog are clusters of galaxies with the mean membership of 36 galaxies. In the catalog, however, are also included smaller groups with the membership of at most 10 galaxies as well as larger structures with the membership of over 100 *clusters*. The mass range of the catalog is thus quite broad from  $10^{12}h^{-1}M_\odot$  to  $10^{16}h^{-1}M_\odot$ .

The SDSS-C4 catalog provides various spectroscopic properties of galaxy clusters, among which the following informations are used for our study: the ratio between the minor and major principal axes ( $q$ ), the r-band luminosity ( $L$ ), the *virial* mass ( $M$ ), and the redshift ( $z$ ). The values of  $M$  and  $L$  depend on the scale of radius ( $w$ ) used to find the member galaxies. In the catalog, there are five different criteria used:  $w = 500, 1000, 1500, 2000,$  and  $2500$  in unit of kpc. For instance, if  $w = 1000$ , it means that all galaxies are included within 1000 kpc from the cluster centers to measure the values of  $M$  and  $L$ . For the detailed descriptions of the C4 catalog and the measurement of  $M$  and  $L$  in the catalog, refer to the web-page of the SDSS-C4 catalog (<http://www.ctio.noao.edu/~chrism/current/research/C4/dr2>).

In this paper, to be consistent, we choose exclusively those values of  $M$  and  $L$  which are measured by using all galaxies within 1000 kpc, because the value of  $q$  of each cluster in the catalog is determined by the criterion of all galaxies within  $w = 1000$  kpc. One thing that has to be mentioned here is that the virial mass,  $M$ , of each cluster in the catalog

was computed under the assumption of a *concordance* cosmology with  $\Omega_m = 0.3$ ,  $\sigma_8 = 0.9$   $h = 0.7$  (the dimensionless hubble parameter). In other words, the cluster mass  $M$  given in the catalog are biased toward the concordance cosmology, which has to be avoided in the parameter estimation (see §4).

Figure 1 plots the distributions of  $q$ ,  $L$ ,  $M$ , and  $z$  of the SDSS-C4 clusters as histograms in the upper left, upper right, lower left, and lower right panels, respectively. The mean value of  $q$  is found to be  $\bar{q} = 0.63 \pm 0.18$ , which indicates that the shapes of galaxy clusters deviate significantly from spherical symmetry. As can be seen, most of the systems in the catalog are clusters whose mass is in the narrow range of  $[-0.5, 1]$  in unit of  $10^{14}h^{-1}M_\odot$ .

We also investigate how the cluster axis-ratio changes with the cluster mass and luminosity by computing the average,  $\bar{q}$  as a function of  $M$  and  $L$ . Figure 2 plot  $\bar{q}(M)$  (upper panel) and  $\bar{q}(L)$  (lower panel) as histograms, respectively. The errors are computed as  $[(\langle q^2 \rangle - \bar{q}^2)/N]^{1/2}$  where  $N$  is the number of galaxy clusters in each bin.

As one can see,  $\bar{q}$  increases with  $M$  and  $L$ . In other words, the more massive and luminous a cluster is, the rounder is its shape. This result from the SDSS-C4 catalog is in direct contrast with that from recent N-body simulations (Hopkins, Bahcall & Bode 2005) where the more massive clusters were found to be more elliptical. However, this observational result is quite consistent with the LJS05 analytic prediction that the more massive clusters are more rounder. We suspect that this inconsistency between simulations and observations must be caused by the different way of identifying clusters. As we are going to compare the observational result not with the numerical one but with the analytic distribution which predicts a consistent trend, we postpone our concerns about this discrepancy till §5.

### 3. PHYSICAL ANALYSIS

#### 3.1. Overview of the Analytic Model

The LJS05 analytic model for the axis-ratio distribution of dark halos adopts two classical theories as its background: the Zel'dovich approximation (Zeldovich 1970) and the density peak formalism (Bardeen et al. 1986).

By applying the Zel'dovich approximation, LJS05 assumed that the three principal axes of a triaxial halo,  $\{a, b, c\}$  (with  $a \leq b \leq c$ ) are related to the eigenvalues of the linear deformation tensor (defined as the second derivative of the perturbation potential),  $\{\lambda_1, \lambda_2, \lambda_3\}$ , as

$$a \propto \sqrt{1 - D_+ \lambda_1}, \quad b \propto \sqrt{1 - D_+ \lambda_2}, \quad c \propto \sqrt{1 - D_+ \lambda_3}, \quad (1)$$

where  $D_+ = D_+(z)$  is the growth rate of the linear density field. Here, the sum of the three eigenvalues equals the linear overdensity,  $\delta$ :  $\lambda_1 + \lambda_2 + \lambda_3 = \delta$ .

By employing the density peak formalism, LJS05 also assumed that a region in the linear density field will condense out a virialized halo if it satisfies the following two conditions:

$$\delta = \delta_c = \delta_{c0} D_+(0)/D_+(z), \quad (2)$$

$$\lambda_3 > \lambda_0 = \lambda_{c0} D_+(0)/D_+(z), \quad (3)$$

where  $\delta_{c0} \equiv \delta_c(0)$  and  $\lambda_{c0} \equiv \lambda_c(0)$ . Basically, equations (2) and (3) represent the *peak* and the local *maxima* conditions in the linear density field, respectively. The value of  $\delta_{c0}$  can be theoretically evaluated by the top-hat spherical collapse model. For instance,  $\delta_{c0} \approx 1.686$  for a flat universe with closure density (e.g., Kitayama & Suto 1996).

As for the value of  $\lambda_{c0}$ , it is precisely 0 in the original density peak formalism. Instead of using this theoretical value, however, LJS05 used a positive value of  $\lambda_c = 0.37$  which was determined empirically through fitting. Their claim was that the break-down of the linear theory in highly nonlinear regime is responsible for the deviation of  $\lambda_{c0}$  from the theoretical value of 0 in practice.

Here, we use the theoretical value of  $\lambda_{c0} = 0$  rather than the empirical value of  $\lambda_{c0} = 0.37$  for the following reason. The value of  $\lambda_{c0} = 0.37$  was found empirically by comparing the analytic model with the *numerical* result on a *galaxy group scale* for the concordance cosmology only. Remember that our purpose is to compare the analytic distribution with the *observational* data on the *galaxy cluster scale* and to probe cosmology without having any bias. As we noticed in §2, the observational and numerical findings are inconsistent with each other. Besides, the density peak formalism and the Zel'dovich approximation may be still valid on quasi-linear regimes, where the galaxy clusters are supposed to stay even at present epoch. Hence, we set  $\lambda_{c0}$  at the original theoretical value 0 in the rest of this paper.

Defining two real variables  $\mu_1$  and  $\mu_2$  as

$$\mu_1 \equiv \frac{b}{c}, \quad \mu_2 \equiv \frac{a}{c}. \quad (4)$$

LJS05 derived analytically the joint probability density distribution of  $\mu_1$  and  $\mu_2$  which depends on the cluster mass  $M$  and the formation epoch  $z_f$ :

$$\begin{aligned} p(\mu_1, \mu_2; M, z_f) &= \frac{3375\sqrt{2}}{\sqrt{10\pi}\sigma_M^5} \exp \left[ -\frac{5\delta_c^2}{2\sigma_M^2} + \frac{15\delta_c(\lambda_1 + \lambda_2)}{2\sigma_M^2} - \frac{15(\lambda_1^2 + \lambda_1\lambda_2 + \lambda_2^2)}{2\sigma_M^2} \right] \\ &\times (2\lambda_1 + \lambda_2 - \delta_c)(\lambda_1 - \lambda_2)(\lambda_1 + 2\lambda_2 - \delta_c) \\ &\times \Theta \left( \frac{1}{D_{+f} - \lambda_1} \right) \Theta[\delta_c - (\lambda_1 + \lambda_2)] \left| \frac{(\partial\lambda_1\partial\lambda_2)}{(\partial\mu_1\partial\mu_2)} \right|, \end{aligned} \quad (5)$$

where  $D_{+f} \equiv D_+(z_f)$ ,  $A$  is the normalization factor, and  $\sigma$  is the standard variation of the linear density field.

The relation between  $\{\mu_1, \mu_2\}$  and  $\{\lambda_1, \lambda_2\}$  are given as

$$\lambda_1 = \frac{1 + (D_{+f}\delta_c - 2)\mu_2^2 + \mu_1^2}{D_{+f}(\mu_1^2 + \mu_2^2 + 1)}, \quad (6)$$

$$\lambda_2 = \frac{1 + (D_{+f}\delta_c - 2)\mu_1^2 + \mu_2^2}{D_{+f}(\mu_1^2 + \mu_2^2 + 1)}, \quad (7)$$

and the Jacobian  $\left| \frac{(\partial\lambda_1\partial\lambda_2)}{(\partial\mu_1\partial\mu_2)} \right|$  was found to be

$$\left| \frac{(\partial\lambda_1\partial\lambda_2)}{(\partial\mu_1\partial\mu_2)} \right| = \frac{4(D_{+f}\delta_c - 3)^2\mu_1\mu_2}{D_{+f}^2(\mu_1^2 + \mu_2^2 + 1)^3}. \quad (8)$$

Equation (5) gives the probability distribution of the two axis-ratios of a triaxial galaxy cluster with mass  $M$  formed at  $z_f$ . In practice, however, we are unable to measure the formation epoch,  $z_f$ . What we can measure in observation is only the observation epoch,  $z$ , i.e., the redshift at which a cluster is observed. Hence, LJS05 rederived an analytic expression for  $p(\mu_1, \mu_2; M; z)$  from equation (5) as

$$p(\mu_1, \mu_2; M; z) = \int_z^\infty dz_f \frac{\partial p_f(z_f; 2M, z)}{\partial z_f} p(\mu_1, \mu_2; 2M; z_f), \quad (9)$$

where  $\partial p_f/\partial z_f$  represents the formation epoch distribution of galaxy clusters. LJS05 used the fitting formula given by Kitayama & Suto (1996) which is an approximation to the analytic expression found by Lacey & Cole (1994).

### 3.2. Projection onto the Sky

Although equations (5)-(9) provides a complete analytic expression for the axis-ratio distribution of the *three dimensional* shape of a triaxial cluster with mass  $M$  observed at  $z$ , it is hard to compare it directly with the observational data. In observation, as we noted in §2, what is measured is only the *two dimensional* projected profiles of galaxy clusters. For a fair comparison of the analytic distribution with the observational data, one should consider the projection of the analytic distribution .

To incorporate into equation (9) the projection effect onto the plane of the sky, we follow Binney (1985): Let  $(\theta, \phi)$  be the usual polar coordinates of the line-of-sight vector in the principal axes of a triaxial cluster, and let  $q$  be the axis-ratio of a two dimensional cluster

profile projected along the line of sight direction. Then, the probability density distribution of  $q$  can be obtained by performing an integration of equation (5) over  $\mu_1, \mu_2, \theta, \phi$  as

$$p(q; M, z) = \frac{1}{4\pi} \int_0^{2\pi} d\phi \int_0^\pi \sin \theta d\theta \int_{\mu_2}^1 d\mu_1 \int_0^1 d\mu_2 \delta_D[q - q'(\theta, \phi, \mu_1, \mu_2)] p(\mu_1, \mu_2; M, z), \quad (10)$$

where

$$q'(\theta, \phi, \mu_1, \mu_2) = \left\{ \frac{U + V - [(U - V)^2 + W^2]^{1/2}}{U + V + [(U - V)^2 + W^2]^{1/2}} \right\}^{1/2}, \quad (11)$$

and

$$U \equiv \frac{\cos^2 \theta}{\mu_2^2} \left( \sin^2 \theta + \frac{\cos^2 \phi}{\mu_1^2} \right) + \frac{\sin^2 \theta}{\mu_1^2}, \quad (12)$$

$$W \equiv \cos \theta \sin 2\phi \left( 1 - \frac{1}{\mu_1^2} \right) \frac{1}{\mu_2}, \quad (13)$$

$$V \equiv \left( \frac{\sin^2 \phi}{\mu_1^2} + \cos^2 \phi \right) \frac{1}{\mu_2^2} \quad (14)$$

Through equations (5)-(10), one can evaluate analytically the probability density that the projected profile of a galaxy cluster of mass  $M$  is observed to have an axis-ratio of  $q$  at redshift  $z$ .

Fig. 4 plots equation (10) on *cluster scale*,  $M_8$ , (see §4 for a definition of  $M_8$ ) at present redshift ( $z = 0$ ) for four different cosmological models: a  $\Lambda$ CDM model with  $\Omega_m = 0.3, \Omega_\Lambda = 0.7, \sigma_8 = 0.9, h = 0.7, \Gamma = 0.168$  (solid line); OCDM model with  $\Omega_m = 0.3, \Omega_\Lambda = 0, \sigma_8 = 0.87, h = 0.83, \Gamma = 0.25$  (dotted); SCDM model with  $\Omega_m = 1, \Omega_\Lambda = 0, \sigma_8 = 0.55, h = 0.55, \Gamma = 0.5$  (dashed);  $\tau$ CDM model with  $\Omega_m = 1, \Omega_\Lambda = 0, \sigma_8 = 0.52, h = 0.5, \Gamma = 0.25$  (long-dashed). Here,  $\Gamma$  is a shape factor related to  $\Omega_m, h$ , and the baryon density parameter,  $\Omega_b$  (e.g., see Peacock & Dodds 1994).

As one can see, equation (10) depends sensitively on the background cosmology. More elliptical clusters are predicted by the  $\Lambda$ CDM and OCDM models with high  $\sigma_8$  and low  $\Omega_m$  than by the SCDM and  $\tau$ CDM models with low  $\sigma_8$  and high  $\Omega_m$ . It can be understood given that the SCDM and  $\tau$ CDM models predict more small scale powers which could result in rounder shapes of galaxy clusters in the end.

We examine the validity of equation (10) by testing it against the observational data, for the case of a concordance cosmology. The testing results are shown in Figures 4 and 5. Figure 4 plots together the analytic (solid line) and the observational (dots) axis-ratio distributions of galaxy clusters for comparison. The errors of the observational points are Poissonian. Figure 5 plots the analytic and the observational mean values of the axis-ratios

as a function of mass. The value of  $z$  in the analytic axis-ratio distribution (eq.[10]), is set at the median redshift of the catalog,  $z_{med} = 0.08$ , to be consistent with the observational data. As one can see, the overall agreement between the analytic and the observational results are remarkably good. Note that the analytic model predicts the increase of the cluster axis-ratios with mass, in good agreement with the observational data. We also evaluate analytically the mean axis-ratio of a typical galaxy cluster by equation (10), and find that  $\bar{q} \approx 0.67$ , which agrees with the observation mean axis ratio (see §2),  $\bar{q}_{ob} = 0.63 \pm 0.18$ , quite well.

## 4. APPLICATION OF THEORY TO OBSERVATIONS

### 4.1. Characteristic Cluster Mass

The analytic axis-ratio distribution (eq.[10]) depends on the cluster mass  $M$  and redshift  $z$ . Therefore, to compare it with the observational data, one has to first specify the values of  $M$  and  $z$ . As for  $z$ , to be consistent with the observational data, we set it at the median redshift of the SDSS-C4 catalog, 0.08, given that the redshift range of the catalog is quite narrow,  $0.03 \leq z \leq 0.17$ .

As for  $M$ , however, one should not set it at the median cluster mass of the catalog for the following reason. As mentioned in §2, the mass of each cluster in the catalog is measured under the assumption of concordance universe. Thus, if we set  $M$  in equation (10) at the median cluster mass of the catalog, the analytic distribution would already assume a bias toward the concordance cosmology. To prevent this kind of bias from the parameter estimation, we set  $M$  not at the median cluster mass of the catalog but at the *characteristic mass scale*,  $M_8$ , defined as

$$M_8 = \frac{4\pi}{3}\bar{\rho}R_8^3, \quad (15)$$

where  $R_8 = 8h^{-1}\text{Mpc}$  is the top-hat spherical radius on which scale the rms mass density variation is *observed* to be very close to unity, and  $\bar{\rho} = 2.78 \cdot 10^{11}\Omega_m h^2 M_\odot \text{Mpc}^{-3}$  is the mean mass density of the universe. Since the galaxy clusters are the largest collapsed objects in the universe, the characteristic mass scale  $M_8$  is believed to represent the typical mass of galaxy clusters. Note that this characteristic cluster mass,  $M_8$ , by its definition (eq.[15]), depends on the value of  $\Omega_m$ . Therefore, if we put  $M = M_8$  into equation (10), it means that the cluster mass  $M$  is not held at some fixed value but varies with the cosmological parameters, which we believe will optimize the parameter estimation without bearing any bias toward a certain cosmology.



#### 4.2. Constraint on $\Omega_m$ and $\sigma_8$ for a Flat Universe

The analytic distribution (10) depends not only on  $\Omega_m$  and  $\sigma_8$  but also on  $\Omega_\Lambda$ ,  $h$ , and  $\Gamma$  as well. Here, we focus mainly on constraining  $\Omega_m$  and  $\sigma_8$ , assuming that the other parameters are already known as priors. We use the following priors from the CMB observation (e.g., Lange et al. 2001), the HST Key Project (Freedman et al. 2001) and the big bang nucleosynthesis (Olive, Steigman, Walker 2000):  $\Omega_\Lambda = 1 - \Omega_m$  (a flat universe);  $h = 0.7$ ;  $\Omega_b = 0.044$ . Once the values of  $h$  and  $\Omega_b$  are given, the shape factor,  $\Gamma$ , will depend only on the value of  $\Omega_m$ .

Now that all parameters except for  $\Omega_m$  and  $\sigma_8$  in equation (10) are prescribed, we can fit the observational data points obtained in §2 to equation (10) with adjusting  $\Omega_m$  and  $\sigma_8$  in ranges of  $(0, 1]$  and  $(0, 2]$ , respectively. We pick as the best-fit values of  $\Omega_m$  and  $\sigma_8$  those that minimize  $\chi^2$  defined as:

$$\chi^2 = \sum_{i=1}^{N_p} \frac{[p_{ob}(q_i) - p(q_i; M_8, z_m)]^2}{\sigma_{ob}^2(q_i)}, \quad (16)$$

where  $N_p$  is the total number of observational data points,  $\{q_i, p_{ob}(q_i)\}$ , and  $\sigma_{ob}(q_i)$  is the observational standard variation of  $q_i$  (see §2).

The best-fit values are found to be  $\Omega_m = 0.48$  and  $\sigma_8 = 0.95$ . This single best-fit values, however, are unreliable given the uncertainty in  $\chi^2$  due to the strong correlation between  $\Omega_m$  and  $\sigma_8$ . A more general best-fit is defined as the full range of the outer limit of one standard deviation contour. Figure 6 plots the one standard deviation contour as solid line. We find that this contour is well approximated as the relation,  $\sigma_8 = (0.99 \pm 0.07)\Omega_m^{(0.07 \pm 0.02) + 0.1\Omega_m}$ . This approximation formula is also plotted as dot-dashed line in Figure 6. The previous relation of  $\sigma_8 = (0.52 \pm 0.04)\Omega_m^{-0.52 + 0.13\Omega_m}$  obtained by Eke, Cole, & Frenk (1996) from the cluster abundance is also plotted for comparison as dashed line. The shaded area surrounded by the solid and the dashed lines in Figure 6 represents the simultaneously constrained best-fit values of  $\Omega_m$  and  $\sigma_8$ :  $\Omega_m^{cons} = 0.31 \pm 0.06$  and  $\sigma_8^{cons} = 0.92 \pm 0.05$ , which is in good agreement with the results from the first year *WMAP* (Wilkinson Microwave Anisotropy Probe) measurements (Spergel 2003).

### 5. DISCUSSION AND CONCLUSIONS

We have found a new  $\sigma_8$ – $\Omega_m$  relation by comparing the analytic axis-ratio distribution of galaxy clusters with the observational data from the SDSS-C4 catalog.

It is, however, worth noting that this new  $\sigma_8$ – $\Omega_m$  relation is subject to one unjustified

assumption that the LJS05 analytic model is valid. LJS05 tested their analytic model against N-body simulations on scales of galaxy groups, and found that although it reproduced some important characteristics of the numerical results, it predicted the increase of the mean axis-ratio with halo mass inconsistent the numerical trend.

Despite that the LJS05 model did not pass N-body test, we have found here that it agrees with the observational results quite well (see Figs. 4 and 5). Especially, the mean axis-ratio of galaxy clusters from the SDSS-C4 catalog, as shown in Figure 5, is shown to increase with mass (and also with luminosity), just as the LJS05 model predicts. Furthermore, the increase of the mean axis-ratio with mass and luminosity is also observed on smaller galaxy scale (M. Strauss 2005, private communication).

We suspect that this discrepancy between simulations and observations may be due to a different way of cluster-identification. In simulations, clusters are identified by the friends-of-friends (FOF) algorithm which uses the separation length between particles as a selection criterion. As a result, the cluster halos identified in simulations by the FOF algorithm tend to be elongated along filaments connecting the neighbor halos (Kim, J. H. 2005, in private communication). On the contrary, observations use the mean spherical overdensity as a selection criterion, which might cause the shapes of galaxy clusters in observations to look rounder. Moreover, the difference between simulations and observations should become larger in the high-mass scale because the filamentary networks get more sharpened in the higher mass scale. In other words, the increase of the cluster ellipticity found in N-body simulations may be due to the increase of the filamentarity of the density field.

A tough question remains: which is a better way to identify a cluster ? In an idealistic theory, galaxy clusters are defined as the largest *virialized* objects in the universe. However, it is very hard in practice to identify clusters using this idealistic virialization condition. We merely assume that the objects selected by a simple scheme like FOF or SO should be more or less virialized. As Suto (2002) pointed out, it will be definitely necessary to find a consistent cluster-identification algorithm for the use of galaxy clusters as a cosmological probe. However, this task is definitely beyond the scope of this paper.

Finally, we conclude that it is possible in principle to constrain both  $\Omega_m$  and  $\sigma_8$  concurrently from the observation of galaxy clusters alone, as the cluster shape and abundance distributions provide two different  $\sigma_8$ - $\Omega_m$  relations. The amplitude of the linear power spectrum obtained from the shape and abundance distribution of the galaxy clusters is consistent with the high value estimated from the recent *WMAP* measurements.

We acknowledge stimulating discussions with M. Im, C.Park, Y.Jing, and R. Sheth. We also thank C. Park, Y. Choi, H. Hwang, J. J. Lee for many helps. This work is supported

by the research grant No. R01-2005-000-10610-0 from the Basic Research Program of the Korea Science and Engineering Foundation.

## REFERENCES

- Bardeen, J. M., Bond, J. R., Kaiser, N., & Szalay, A. S. 1986, *ApJ*, 304, 15
- Binney, J. 1985, *MNRAS*, 212, 767
- Bond, J. R., & Myers, S. T. 1996, *ApJS*, 103, 63
- Bond, J., R., Kofman, L., & Pogosyan, D. 1996, *Nature*, 380, 603
- Carlberg, R. G. et al. 1996, *ApJ*, 462, 32
- de Bernardis, P. et al. 2000, *Nature*, 404, 955
- Eke, V. R., Cole, S., & Frenk C. S. 1996, *MNRAS*, 282, 263
- Fan, Z., & Chiueh, T. 2001, *ApJ*, 550, 547
- Freedman, W. L., et al. 2001, *ApJ*, 553, 47
- Henry, J. P. & Arnaud, K. A. 1991, *ApJ*, 372, 410
- Henry, J. P. 2000, *ApJ*, 534, 565
- Hopkins, P. F., Bahcall, N., & Bode, P. 2005, *ApJin press*
- Jing, Y. P. & Suto, Y. 1998, *ApJ*, 503, L9
- Jing, Y. P. & Suto, Y. 2000, *ApJ*, 529, L69
- Kitayama, T. & Suto, Y. 1996, *ApJ*, 469, 480
- Lacey, C. & Cole, S. 1994, *MNRAS*, 271, 676
- Lange, A. E. et al. 2001, *Phys. Rev. D.*, 63, 042001
- Lee, J., Jing, Y., & Suto, Y. 2005, *ApJin press*
- Miller, C. J., et al. 2005, *AJin press* [astro0poh/0503713]
- Olive, K. A., Steigman, G., Walker, T. P. 2000, *Phys. Rep.*, 333, 389
- Peacock, J. A., & Dodds, S. J. 1994, *MNRAS*, 267, 1020
- Pen, U. L. 1998, *ApJ*, 498, 60
- Pierpaoli, E., Scott, D., & White, M. 2001, *MNRAS*, 325, 77

- Press, W., & Schechter, P., 1974, ApJ, 187, 425
- Rasia, E., et al. 2005, ApJ, 618, L1
- Seljak, U. 2002, MNRAS, 337, 769
- Spergel, D. N. et al. 2003, ApJ, 148, 175
- Springel, V., White, S. D. M., Tormen, G., Kauffmann, G. 2001, MNRAS, 328, 726
- Strauss, M. A. et al. 2002, AJ, 124, 1810
- Suto, Y. 2002, AMiBA 2001: High-z Clusters, Missing Baryons, and CMB Polarization”,  
(San Francisco : A. D. P. CONF. SER.), 257, 195
- West, M. J. 1989, ApJ, 347, 610
- White, S. D. M., Efstathiou, G., Frenk, C. S. 1993, MNRAS, 262, 1023
- Zel’dovich, Y. B. 1970, A& A, 5, 84

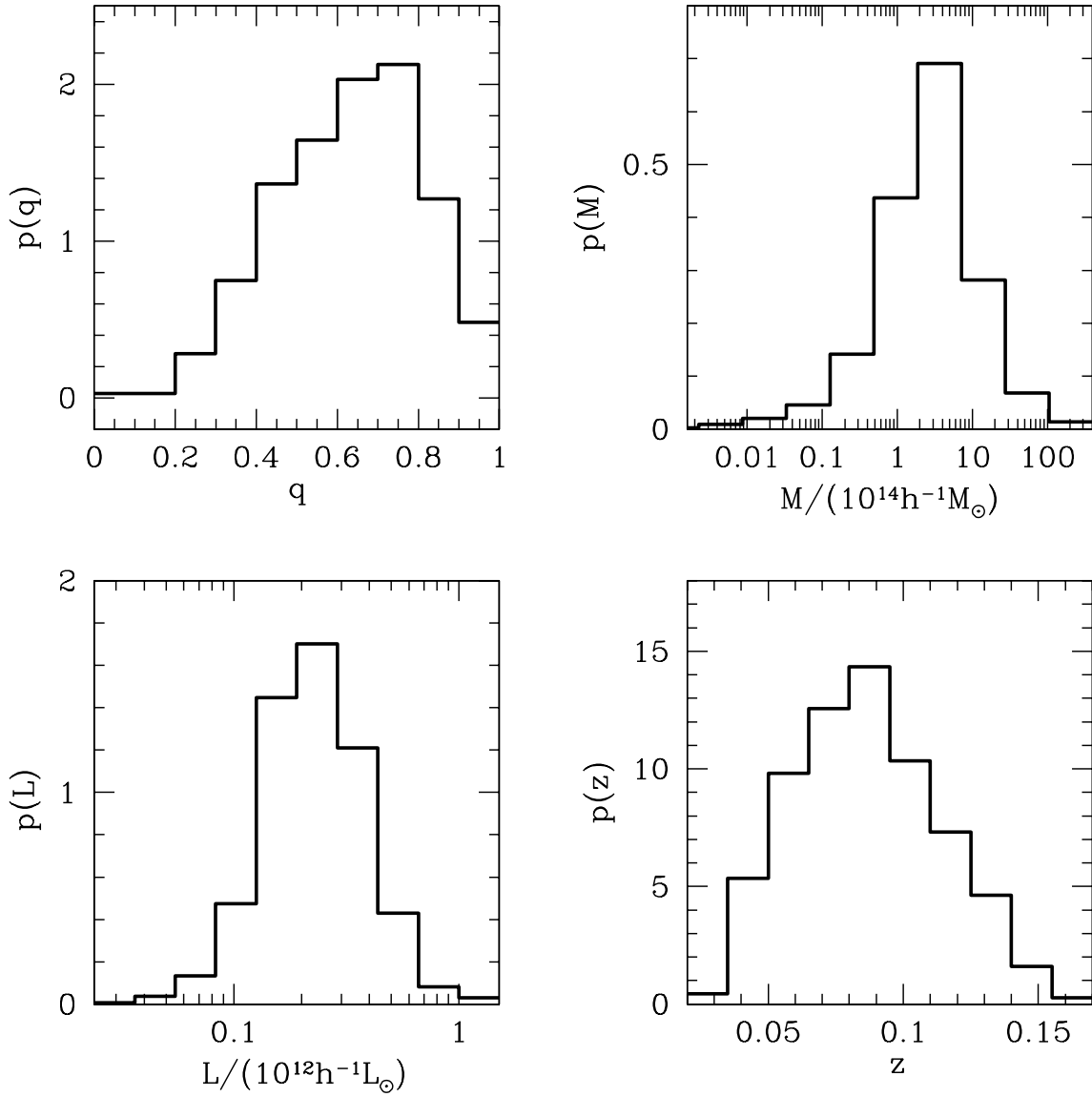


Fig. 1.— Histograms of the probability densities of four different properties of the SDSS-C4 clusters: *Upper left*: the axis-ratio; *Upper right*: the mass; *Lower left*: the luminosity; *Lower right*: the redshift.

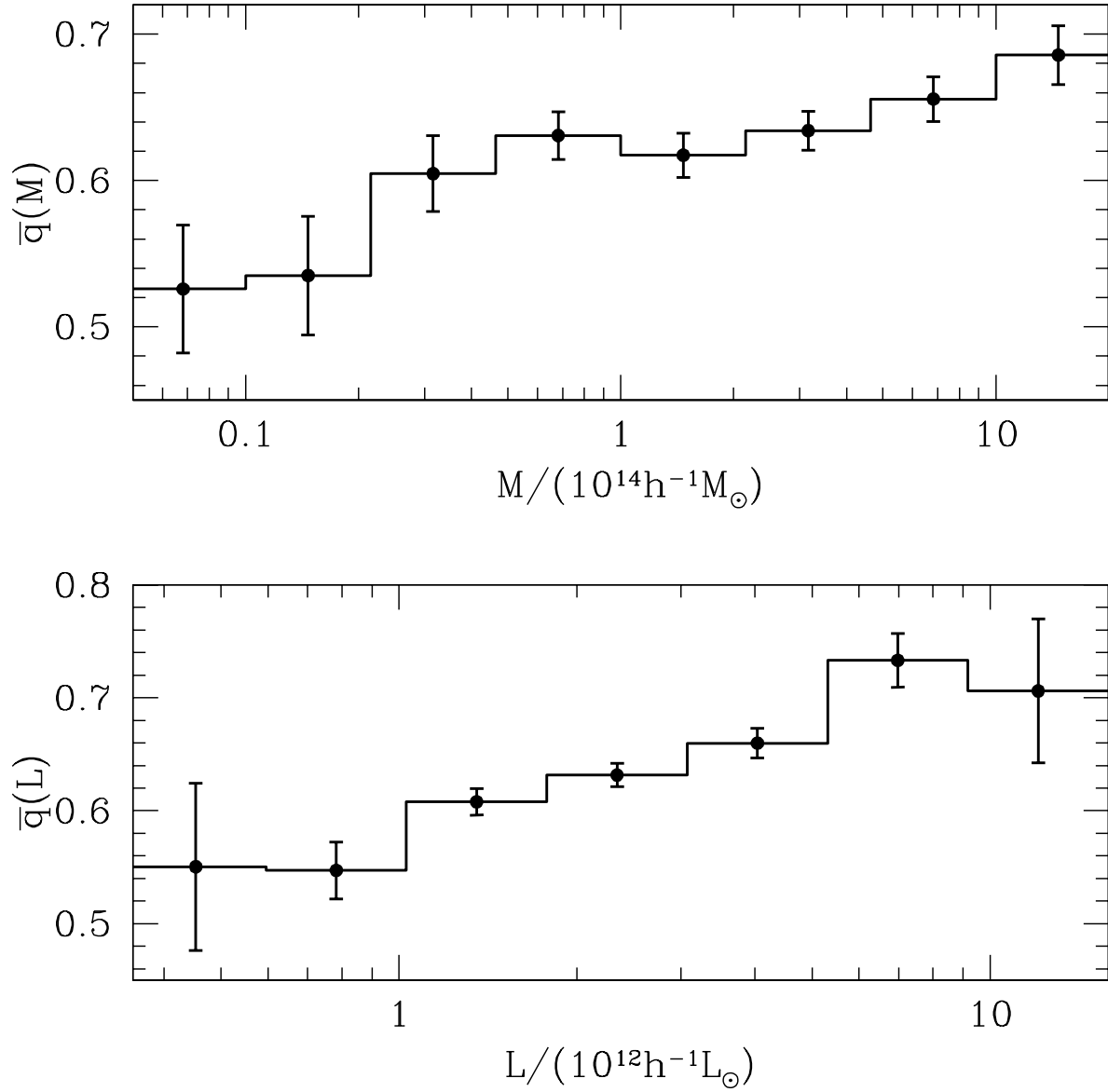


Fig. 2.— The mean axis-ratio of the SDSS-C4 clusters as functions of mass (upper panel) and luminosity (lower panel). The errors represent the standard deviations of the axis-ratio.

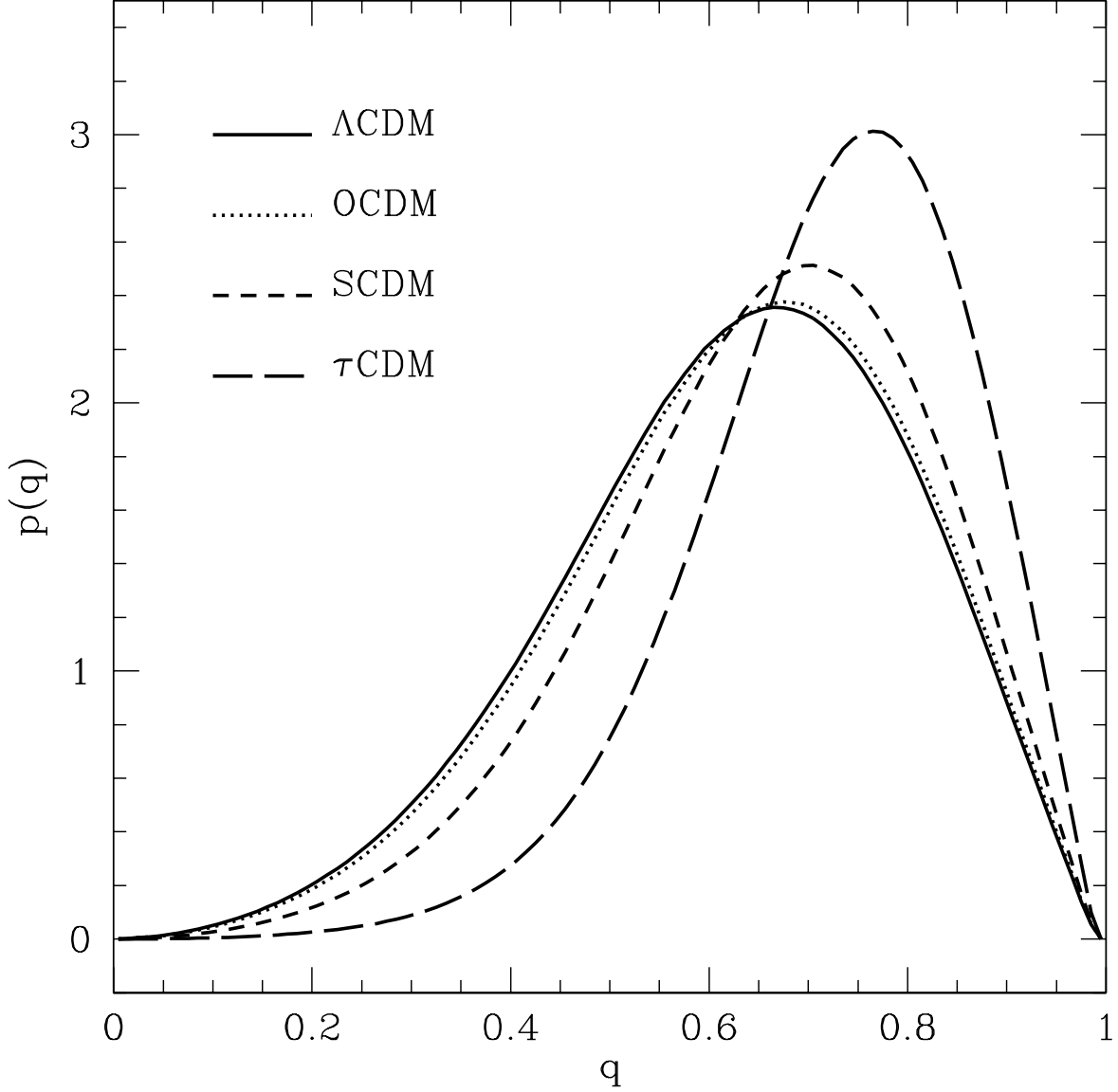


Fig. 3.— The axis-ratio distributions of the two dimensional projected profiles of galaxy clusters predicted by the analytic LJS05 model (eq.[10]) at present epoch for four different cosmological models: a  $\Lambda$ CDM model with  $\Omega_m = 0.3$ ,  $\Omega_\Lambda = 0.7$ ,  $\sigma_8 = 0.9$ ,  $h = 0.7$ ,  $\Gamma = 0.168$  (solid line); OCDM model with  $\Omega_m = 0.3$ ,  $\Omega_\Lambda = 0$ ,  $\sigma_8 = 0.87$ ,  $h = 0.83$ ,  $\Gamma = 0.25$  (dotted); SCDM model with  $\Omega_m = 1$ ,  $\Omega_\Lambda = 0$ ,  $\sigma_8 = 0.55$ ,  $h = 0.55$ ,  $\Gamma = 0.5$  (dashed);  $\tau$ CDM model with  $\Omega_m = 1$ ,  $\Omega_\Lambda = 0$ ,  $\sigma_8 = 0.52$ ,  $h = 0.5$ ,  $\Gamma = 0.25$  (long-dashed).



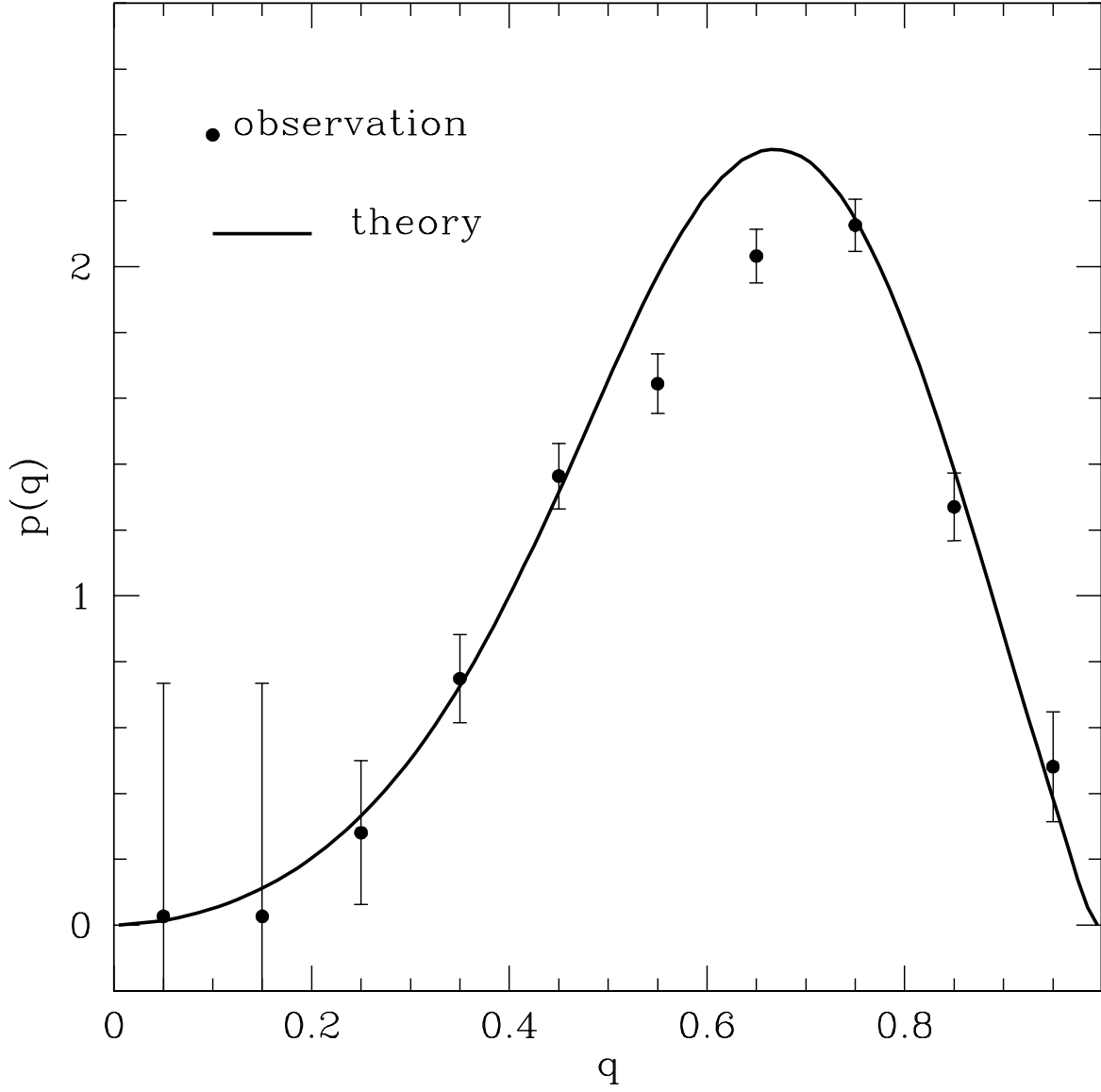


Fig. 4.— The analytic axis-ratio distribution of the two dimensional projected profiles of galaxy clusters (solid line) and the observational data points arising from the SDSS-C4 catalog (solid dots). The errorbars are Poissonian.

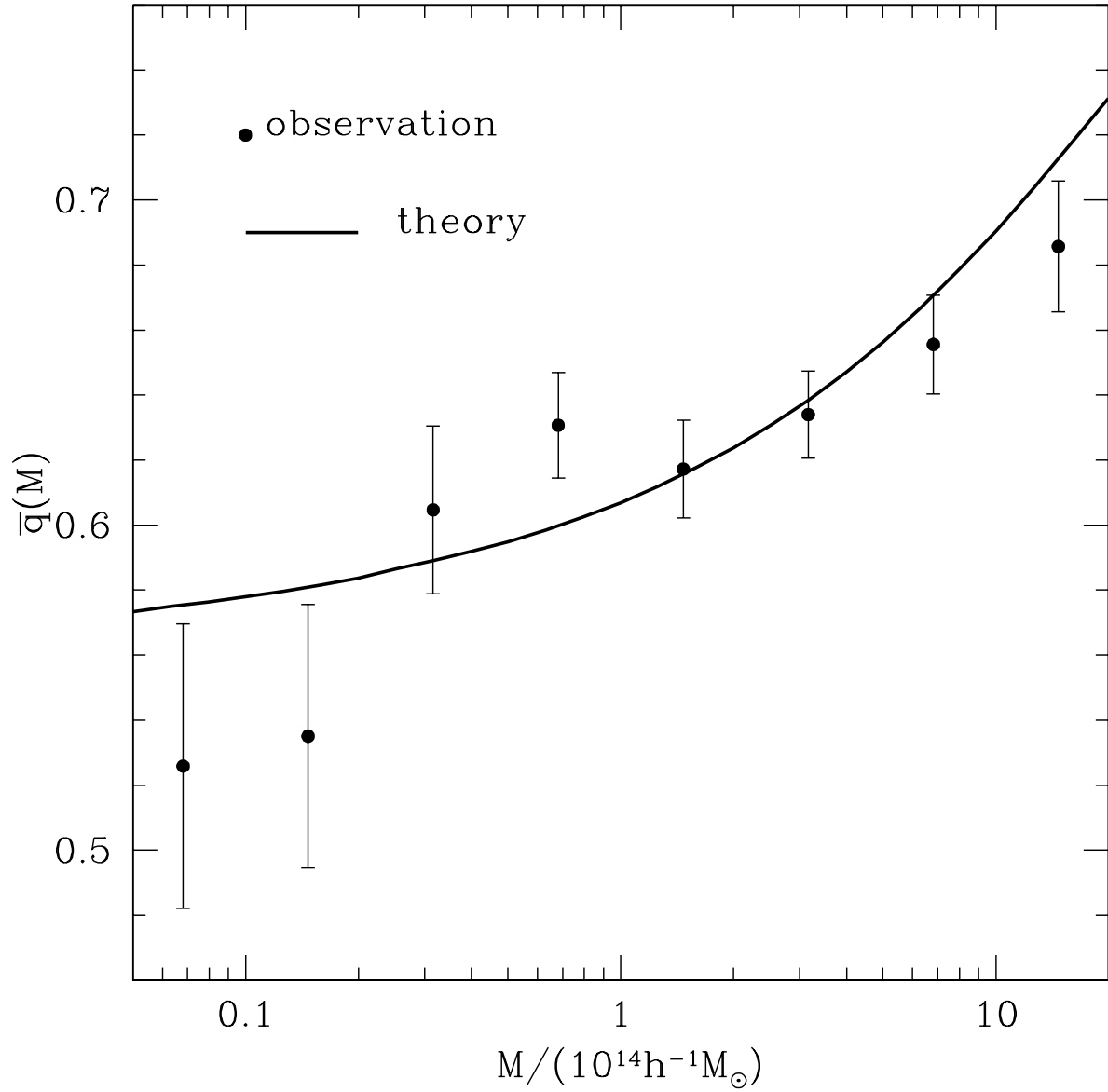


Fig. 5.— The analytic curve for the mean axis-ratio of the two dimensional projected profiles of galaxy clusters as a function of cluster mass (solid line) and the observational data points arising from the SDSS-C4 catalog (solid dots). The errorbars are Poissonian.

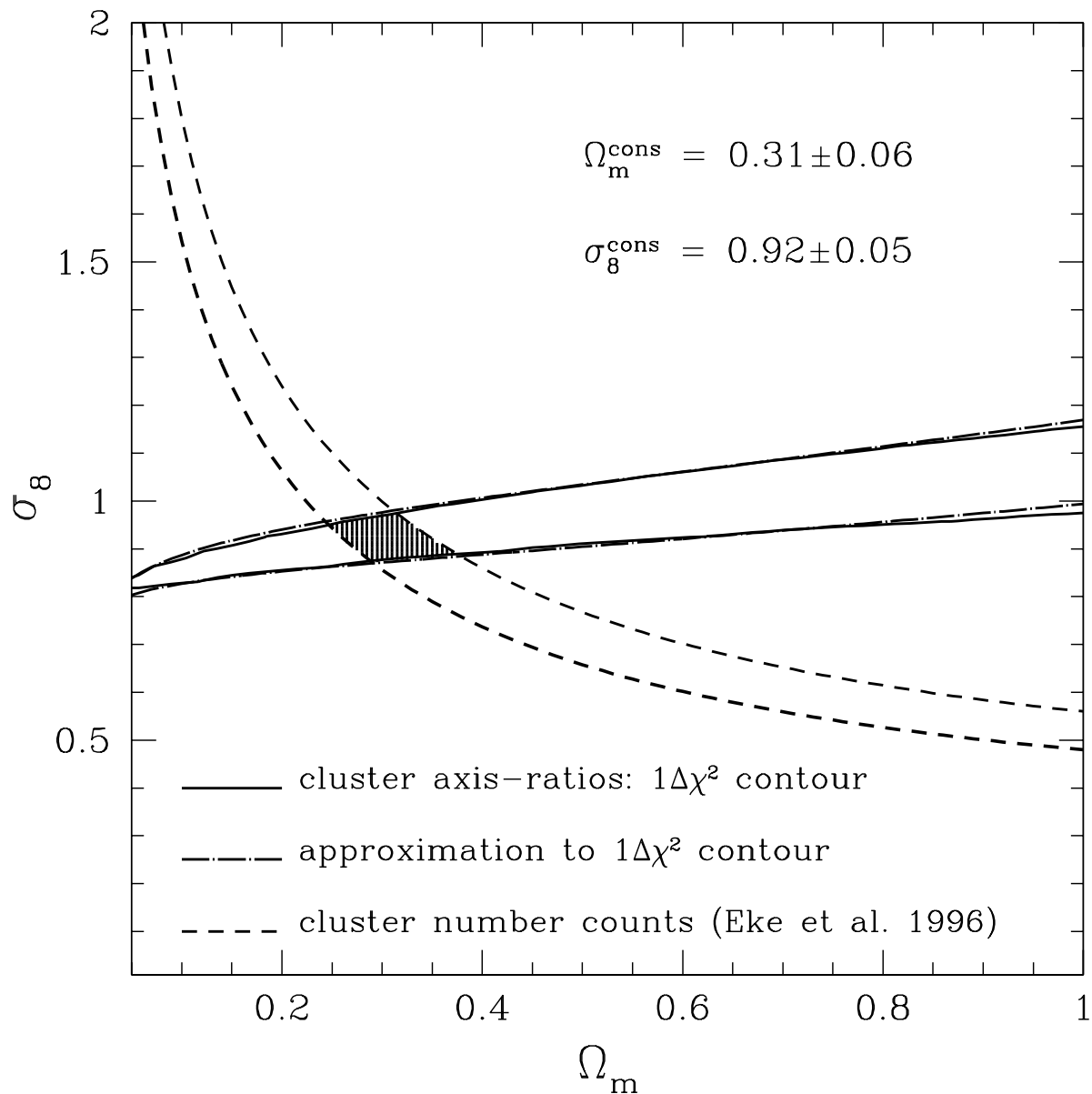


Fig. 6.— The bestfit values of  $\sigma_8$ – $\Omega_m$  through  $\chi^2$ -statistics. The solid and the dot-dashed lines represent the one standard deviation contour and its approximation. The dashed lines is the relation found from the local abundance of X-ray clusters.